Dyes and Pigments 6 (1985) 115–134

Direct Imaging of Organic Molecules in Crystals by High Resolution Electron Microscopy at Atomic Level

Natsu Uyeda

Institute for Chemical Research, Kyoto University,
Uji, Kyoto-Fu 611, Japan

(Received: 2 May, 1984)

SUMMARY

Electron microscopy is a standard technique for the characterization of fine pigment particles. By combined use with electron diffraction, information on crystal structures can be obtained in relation to morphological aspects more accurately than by X-ray powder diffraction. Since the mechanism of image formation by the electron lens follows the same principles of wave summation as structure analysis based on single crystal diffraction, the direct observation of crystal structure is possible if the instrument has the necessary capability and if the specimen is adequately prepared. Electron wave optical theory suggests that the use of shorter wavelengths is the essential approach even to high resolution at the atomic level. By the use of a specially designed high voltage electron microscope, the molecular images of Cyanine Green crystal were observed to give the images due to chlorine and copper atoms in addition to structural details such as azaporphyrin and benzene rings. The application to the conventional case and future prospects are discussed in terms of the radiation damage of ordinary organic compounds.

1. INTRODUCTION

A knowledge of crystal form is one of the most fundamental factors for the characterization of pigment powders. Polymorphic change is known to exert certain effects on the colour characteristics of pigments. For the

Dyes and Pigments 0143-7208/85/$03·30

identification of crystal forms, X-ray powder diffraction is currently adopted even without the information of exact structures. It is interesting to note that X-ray structure analysis in its early days was often concerned with pigment materials; for example, Robertson and coworkers[1] used phthalocyanine derivatives as the specimen crystals for the development of the so-called isomorphic replacement method.

Another fundamental technique of pigment characterization is electron microscopy, which is the only way to study the morphological properties of very fine powder particles. With the transmission mode, crystallographic identification is also possible by means of the selected area diffraction technique (SAD), which may even furnish much better data to detect the structure than those given by ordinary X-ray powder diffraction. The major purpose of structure analysis by X-ray or electron diffraction is to determine the bond lengths and angles of molecules and to 'picturize' the images for better understanding. However, the essential function of electron microscopy is to 'visualize' structural detail by the direct formation of images, the resolution of which may be considered to reach atomic levels if the classical principle of lens optics is regarded as still valid for electrons having wavelengths two digits shorter than ordinary bond lengths in general.

In 1956, lattice fringe images of *ca.* 1 nm spacing were observed by Menter[2] for the first time in needle-like crystallites of phthalocyanine compounds, visually verifying the existing periodicities in crystals. Although no fine structures other than lattice defects were observed, this achievement has been accepted as the first stride taken beyond simple morphological observation towards the visual detection of inner structures. Later, the lattice imaging technique was extended to two-dimensional arrays, the spacings of which finally reached a range less than 0·1 nm by the end of the 1960s, and it was widely applied to practical studies of local fine structures in submicron particles and thin crystalline films.

This steady development proved that the conventional electron microscope had been improved so as to acquire enough efficiency with regard to its mechanical and electrical stabilities. On the other hand, lattice imaging was considered to show only the arrangements of unit cells however small the spacing might be. By adopting a new observation mode called many-beam synthesis, Uyeda *et al.*[3] observed molecular images of Cyanine Green crystallites. Although the result was only to show their cross-like shapes, the new approach was considered to lead to the real

improvement of image resolution to inspect the actual structures within each unit cell.

A wave-optical theory developed by Scherzer[4] suggested that resolving power would be increased by reducing the wavelength rather than by improving the efficiency of the electron lens. Since the shorter wavelengths can be obtained only by increasing the accelerating voltage of the electrons, a new high voltage electron microscope operating at 500 kV was constructed by Kobayashi *et al.*[5] in 1974 to attain the resolving power of 0·14 nm, which is almost of the same order as the ordinary bond length and atomic diameter. The present paper explains the principle of high resolution image formation and some results which show molecular structures in terms of the atomic arrangement. Future applications will be discussed also for the development of the method as a routine technique for the chemical characterization of materials.

2. THE MECHANISM OF HIGH RESOLUTION IMAGE FORMATION

The formation of electron images is in principle based on a similar mechanism to X-ray diffraction structure analysis in the sense that the diffracted beams contribute to the image formation as the result of two-dimensional wave summation which can be achieved in the case of X-rays only by computerized Fourier synthesis. Figure 1(a) is a schematic drawing of the ray path through an ideal objective lens to show the mechanism of image formation. Actually, a conventional electron microscope has two condenser lenses to illuminate the specimen and a series of lenses which follow the objective lens to project a magnified final image onto the viewing screen or a photographic film. The objective lens, however, is the most important of all and the quality and resolution of the final image is already defined by the efficiency of this lens.

When the specimen crystal is illuminated by the incident beam, which is controlled to be as parallel as possible for standard high resolution work, the constituent atoms scatter electron waves which, conically propagating, interfere with one another to excite diffraction. After passing through the lens, these waves converge at certain positions on the focal plane (D in Fig. 1(a)) to produce a cross-grating pattern when the specimen is a crystal. As shown in Fig. 1(b), for example, the diffraction pattern can be recorded by manoeuvering the successive lens systems. Before high

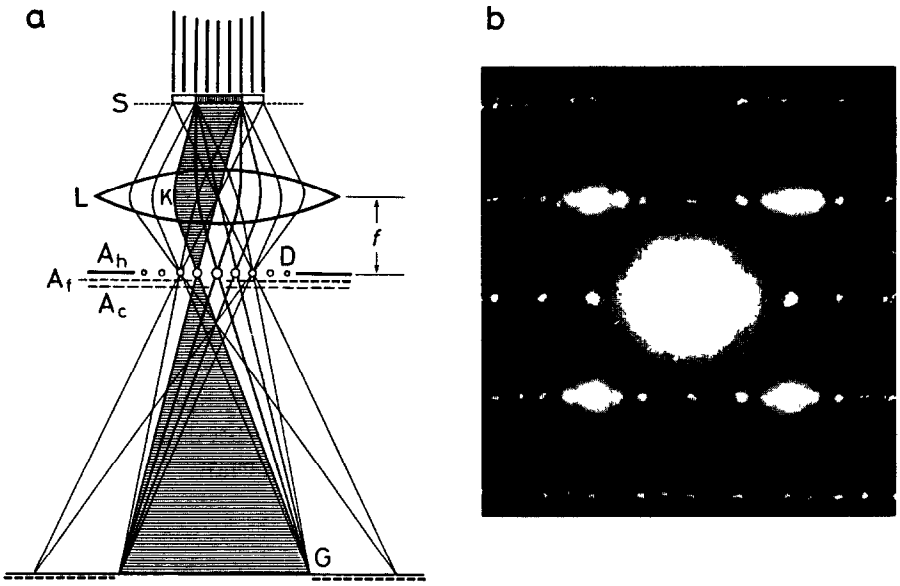

Fig. 1. Function of objective lens for image formation. (a) Ray diagram to show the relationship of diffraction and image. The functions of the objective apertures are as follows: A_c, high contrast observation; A_f, lattice fringe formation; and A_h, high resolution imaging. (b) An example of a selected area diffraction (SAD) pattern obtained from a crystallite of Cu-phthalocyanine of the β-form.

resolution imaging was realized, this procedure (called selected area diffraction) had been the only possible way to obtain structural information on small crystallites under microscopic observation. (One can analyse the structure in the same way as X-ray diffraction by measuring the appropriate intensities and by recovering the phase information lost due to the recording of intensity.) For electron image recording, the diffracted beams, with their individual phases intact, keep propagating in diverging cones to meet altogether at the image plane (G). The summation of all waves produces a two-dimensional amplitude distribution, which is successively magnified and transferred onto the viewing screen or photographic film.

As is well known, the resolving power of a lens, defined as the smallest distance δ between two point objects showing recognizably separated images, is given by the Abbe formula as:

$$\delta = 0{\cdot}65\lambda/\sin\alpha \tag{1}$$

where λ and α are the wavelength and scattering angle of diffracted

electrons. If the bond length can be accepted for δ, the equation is simplified in the electron case to

$$\delta = 0{\cdot}65\lambda/\alpha \tag{2}$$

since the conventional electron wavelength is two digits smaller than δ and α stays effectively in the region of 10–20 mrad at the maximum. Equation (2) indicates that the information on finer structures is conveyed by those waves having reciprocally higher scattering angles. In other words, one must increase the angular range of scattered waves as much as possible in order to attain a higher resolution if the wavelength is kept constant.

Unfortunately, however, the above principle does not apply simply to the case of magnetic electron lenses, as they are not free from various aberrations, among which spherical aberration is known to have a direct influence on the resolving power. In order to avoid the effect of spherical and other aberrations, the objective aperture has been used so as to let only the central scattering through the hole. Although the use of an objective aperture which blocks all the diffracted waves is effective in increasing the contrast and sharpness of the images at medium magnifications, the procedure has followed quite the opposite approach as far as the attainment of high resolution is concerned.

The first step towards direct imaging of crystal structures was taken by Menter,[2] who succeeded in the observation of lattice fringe images by using slender crystallites of phthalocyanine derivatives. In this approach, the main beam was accompanied by another beam of the lowest-scattering angle (e.g. K in Fig. 1(a)), both being let through the objective aperture to interfere with each other at the image plane. Figure 2(a) is an example of lattice fringe images observed by this technique in a Cu-phthalocyanine crystal of β-form, which show a twinned structure consisting of (100) and (20$\bar{1}$) lattice planes of 1·26 and 0·98 nm spacing, respectively. As shown schematically in Fig. 2(b), phthalocyanine crystals are usually composed of columns in which the planar molecules are stacked parallel by the action of π-electronic Van der Waals forces. The fringe image is considered to reflect the parallel arrangement of these columns.

Owing to steady improvement in the instrumentation of electron microscopes, the spacing of lattice fringes to be observed had been reduced year after year, finally reaching a value less than 0·1 nm by the end of the 1960s. In parallel with this development, fringe observation was extended to two-dimensional periodic lattice imaging and has been

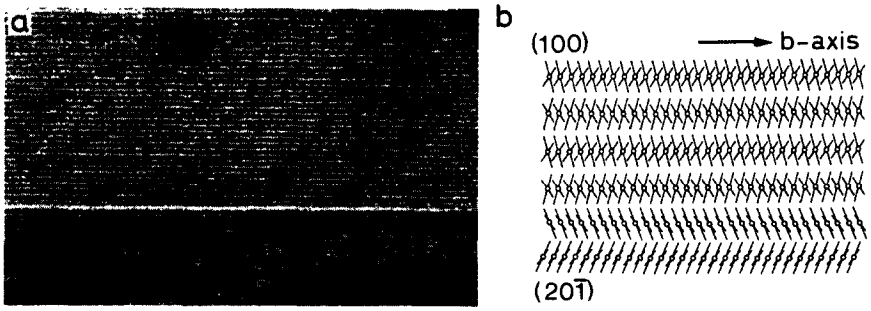

Fig. 2. Lattice fringe images of β-form Cu-phthalocyanine. (a) Electron photomicrograph of twinned lattice structure. (b) Molecular arrangement to form lattice structure of large spacing.

applied to studies of the regular and irregular structures of crystalline materials. However, the images formed by the use of the main and one or two neighbouring waves are known to give only the arrangement of unit cells, however small the fringe spacing might be. If one intends to determine the actual structure in terms of molecular or atomic arrangement, the image should reflect much finer details within each unit cell. For this purpose, the image must be formed not only by using a few waves but by adding as many waves as possible, opening the objective aperture widely so that those waves scattered in higher angular ranges can participate in the image formation through mutual interference. When spherical aberration exists, the waves with higher scattering angle meet the optical axis at positions correspondingly closer to the lens, as shown in Fig. 3. As a result, the image of a point object, for instance, expands to a circle of confusion of radius r, which is proportional to the cube of scattering angle α, so that

$$r = C_s \cdot \alpha^3 \tag{3}$$

where C_s, the spherical aberration constant, is one of the significant characteristics of the objective lens, especially in the case of electron

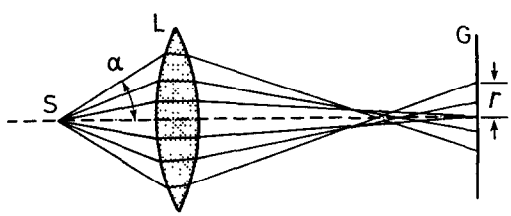

Fig. 3. Spherical aberration of objective lens and least circle of confusion.

microscope. With waves of higher scattering angles, the least circle of confusion increases to degrade the effective resolution while it may not be improved without them (as eqn (1) predicts).

The only possible way to overcome such a dilemma is to find some optimum scattering angle. On the basis of wave optical considerations, Scherzer[4] pointed out that the effect of spherical aberration is mostly to cause the scattered waves to change phase frequently as a function of α and of the focus setting, which can be adjusted by controlling the lens current. According to the theory, there is a definite focus position where the phase of the scattered wave stays intact for a wide angular range (α_{opt}) which is given by

$$\alpha_{opt} = 1{\cdot}41(\lambda/C_s)^{1/4} \tag{4}$$

This particular focus position, often called the Scherzer focus, is found when the focal length is adjusted to be about several tens of nanometres longer than the regular one (underfocus). A new formula for resolving power can be derived for a lens with spherical aberration by combination with eqn (1) as follows:

$$\delta = 0{\cdot}63C_s^{1/4}\lambda^{3/4} \tag{5}$$

The equation indicates that the most efficient way to increase the resolving power is again to reduce the wavelength although the improvement of the spherical aberration cannot be overlooked in spite of its lower efficiency. Since the wavelength of an electron source is inversely proportional to the square root of the accelerating voltage (with the relativistic correction neglected), the adoption of high voltage electron microscopy is considered to be the best direct approach to the attainment of resolving power of atomic order. Technically, however, an undue increase in the voltage does not lead to an ideal result, because the stability of all the electric devices should be better than 1×10^{-6} to avoid the effects of another lens defect called chromatic aberration, which is as serious as spherical aberration for the degradation of image resolution. Apparently, the fluctuation of accelerating voltage causes the electron source to be polychromatic, and that of the lens current results in the fluctuation of focal length.

In 1974, the first high voltage electron microscope (JEM-500) designed especially for atomic resolution was constructed at Kyoto University to operate at 500 kV, which voltage was adopted with engineering capability at that time being taken into account. The wavelength and the spherical

aberration constant are 0·0014 nm and 1·09 nm, respectively, which are supposed to give a resolution of about 0·14 nm when calculated from eqn (5).

3. SPECIMEN PREPARATION

In addition to the attainment of instrumental capability, the method of preparation of specimens is another important factor in high resolution observation of structure images at the atomic level. As already explained, the image is formed by the two-dimensional summation of waves scattered by the constituent atoms. Since the scattering angle is less than 10^{-2} rad, the image is given as a two-dimensional projection of actual structure in the beam direction. Pigment crystals such as phthalocyanines have planar molecules stacked parallel in columns at a definite tilt angle characteristic of the modification.

As illustrated in Fig. 4, the projection onto a plane perpendicular to the column axis would appear as a two-dimensional arrangement of molecules, each of which is a superposition of all the molecules in a column. Although the molecular shape in the projection is slightly deformed due to the tilt, to bring the column axis parallel to the optical axis is the best way to observe the molecular structure image clearly. However, these planar molecules show a strong tendency to pile up in the

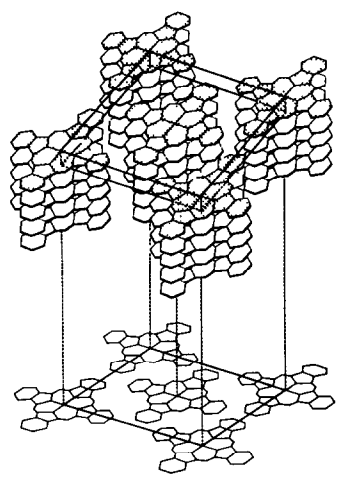

Fig. 4. Molecular column structure and its two-dimensional projection.

column through strong π-electronic interactions, resulting in long needle-shaped crystals which are undesirable not only for pigment production but also for the purpose of molecular image observation. Although thin sectioning normal to the main axis of needles may be considered as a standard method to apply in such a case, the thickness cannot be smaller than 10 nm to fulfil the condition required from a theoretical viewpoint, as will be discussed later.

To overcome this difficulty, the specimens were prepared by vacuum condensation which facilitates thickness determination and at the same time the control of the crystal orientation.

Most phthalocyanines and similar polycyclic pigments can be sublimated at about 400 °C or below in a vacuum lower than 1×10^{-5} Pa. When deposited onto a clean cleavage face of a substrate crystal such as an alkali halide or mica, thin crystalline films are formed by epitaxial growth, as found by Uyeda *et al.*[6] The crystal thickness can be monitored by the use of a quartz crystal microbalance placed near the substrate. After reinforcement with an additional vacuum-deposited thin carbon film, the crystalline film of pigment is stripped off the substrate onto a clean water surface (wet-strip) and transferred to the specimen grid for practical observation.

The crystallites in the epitaxial film of those organic compounds having planar structures assume certain orientations with their molecular column axes standing almost normal to the substrate face, although the exact tilt angle is characteristic of each compound. Figure 5(a) shows an example of epitaxial crystallites of Cu-phthalocyanine grown on KCl. From the analysis of SAD patterns, it can be deduced that the column axis is tilted at 32° to the normal of the substrate face while its projection to the same surface subtends an angle of 20° with the [100] direction of the surface lattice of KCl. In this state, the basal habit face of each crystallite has been found to be the $(31\bar{3})$ plane, to which the planar phthalocyanine molecules are oriented parallel in each crystal.

Taking into account these factors found with various normal metal phthalocyanines, Ashida *et al.*[7] have deduced as a growth mechanism that the orientation adsorption of planar molecules on the substrate lattice defines the epitaxial nucleation as illustrated in Fig. 5(b). The molecule shows a remarkable correlation with the ionic lattice of the substrate KCl, where somewhat strong ion–dipole interactions between the potassium ions and slightly electronegative bridge nitrogen atoms occur. In addition to the normal phthalocyanine derivatives, similar

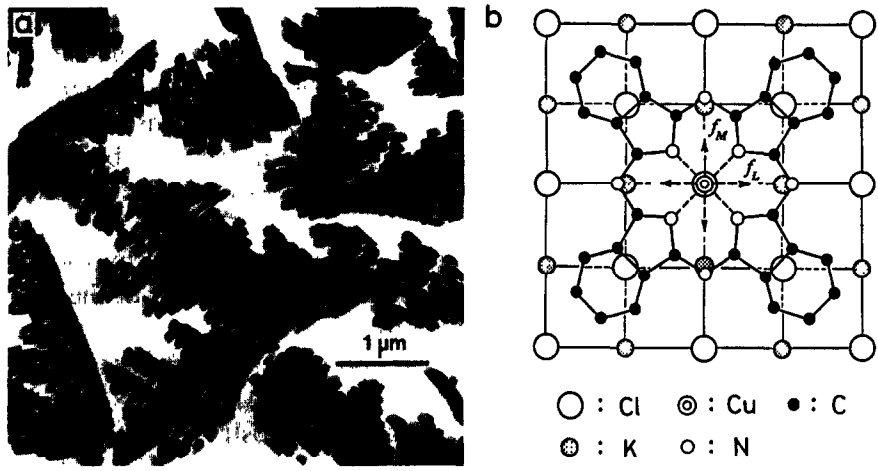

Fig. 5. Epitaxial growth of pigment crystallite on KCl surface. (a) Example of thin α-form Cu-phthalocyanine crystallites with *b*-axis standing almost normal to the basal habit face. (b) Oriented adsorption of single molecule as the epitaxial nucleation on the ionic lattice of KCl (100) face.

epitaxial growth has been observed with various compounds such as 7,7′,8,8′-tetracyanoquinodimethane (TCNQ),[8] tetrahalogenoparaquinones[9] and Th-phthalocyanine.[10] The structures and orientations have been well interpreted in terms of the same mechanism based on the principle of oriented adsorption. The influence of the molecule–substrate interaction is sometimes so strong that even different polymorphs are formed by the effect of the epitaxial growth, as for instance in the case of iodanil.[9] The possibility of the oriented adsorption of π-electronic molecules on the alkali halide surface was confirmed[11] by applying the LEED–Auger technique in regard to tetracyanoethylene and tetrahalogenoethylenes, although the molecule is not so large as a pigment molecule.

It has been shown that a thick specimen is more favourable from the viewpoint of the image intensity and the mechanical strength. However, the necessity of using a thin specimen stems from the characteristic behaviour of electrons, which have a strong capability to interact with atoms. If the crystal thickness is not adequate, the scattered electrons are apt to repeat the scattering (multiple scattering) with atoms during transmission so as to convey confused information to the image plane. Since the diffracted electron waves which are allowed to participate in the appropriate image formation should be those that are singly

scattered, the crystal must be kept as thin as possible to avoid the effect of multiple scattering. The optimum thickness is determined on the basis of the theory developed by Cowley and Moodie[12] as well as by Ishizuka and Uyeda[13] concerning the behaviour of electrons scattered from atoms in a crystal. Generally, thickness can be increased when the energy of electrons is high and the crystal contains only lighter atoms, such as those in organic molecules. The practical calculation shows that the thickness should be in a range of 5–10 nm for most of the phthalocyanines and similar pigments.

4. THE PRACTICAL HIGH RESOLUTION OBSERVATIONS

For the attainment of atomic resolution, the image intensity peaks due to atoms should be as free as possible from the photographic noise of the silver grains in the photographic emulsion. Since the grain size of the developed photograph is nearly 20–30 μm for conventional electron films and the atomic size and distance are of the order of 0·1 nm, the electron optical magnification should be a few hundred thousands or more. Such a high magnification in turn requires a dense electron dose to keep the brightness of the images, giving serious radiation damage to the specimen molecules. Although the effect is more destructive for ordinary organic substances, many π-electronic compounds are known to stand the electron irradiation to a limited extent. However, polyhalogenated metal phthalocyanine (Cyanine Green) was found to be nearly one hundred times more radiation resistant than the ordinary phthalocyanines, indicating that reduction in the number of C—H bonds is effective in increasing the stability to electron irradiation.

In the present work, a commercial product of polychlorinated Cu-phthalocyanine (Heliogen Green 8G) was used as the test specimen. A small amount of powder was evaporated from a quartz crucible heated at 500 °C in a vacuum vessel. The epitaxial film was formed on the fresh (001) cleaved face of KCl. Figure 6(a) is an example of electron photomicrographs of the epitaxial crystallites showing the basal (001) plane. When the goniometer is adjusted to give one of the crystallites a definite tilt angle, the selected area diffraction pattern appears as shown in Fig. 6(b), indicating that the *c*-axis or the column axis is aligned parallel with the incident beam. The rectangular array of the cross-like patterns in Fig. 6(c) shows the molecular images observed for the first time[14] with a

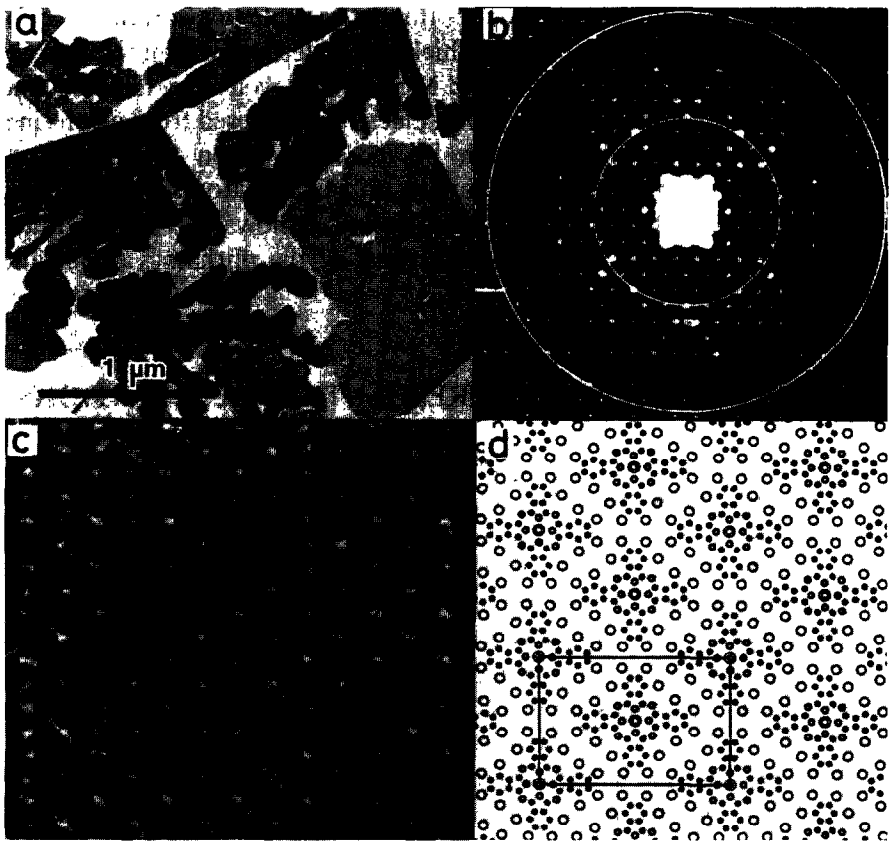

Fig. 6. Crystal structure determination of chlorinated Cu-phthalocyanine (Cyanine Green). (a) Thin crystallite of Cyanine Green epitaxially grown on KCl face. (b) SAD pattern and objective aperture for high resolution imaging. Small circle, molecular imaging; large circle, atomic imaging. (c) Molecular images of Cyanine Green taken with 100 kV instrument. (d) Two-dimensional projection along the column axis of Cyanine Green as determined by the combined analysis of SAD pattern and images.

conventional 100 kV electron microscope by letting the diffracted waves through the aperture indicated by the smaller circle. Although the real molecular arrangement was not known at that time, the crystal structure was analysed on the basis of the diffraction pattern and the general aspect of the molecular images. The crystal data found are as follows: $a = 1{\cdot}962$ nm, $b = 2{\cdot}608$ nm, $c = 0{\cdot}376$ nm, $\beta = 116{\cdot}5°$; monoclinic space group $C2/c$. The projection along the c-axis gives the two-dimensional arrangement as shown in Fig. 6(d).

New molecular images were observed[15] with the 500 kV electron microscope, taking all the diffracted waves within the larger circle of aperture indicated in Fig. 6(b). The number of waves participating in the image formation has been very much increased so as to give finer structural details. The focusing is usually carried out by adjusting the focal length of the objective lens. In the case of high resolution observations, a throughfocus series of the same image field must be recorded by changing the focus in constant steps. The present specimen, however, must be held in the goniometer in a position tilted at nearly 25° for the *c*-axis to be parallel to the incident beam. This situation gives a linear variation in the distance of the object from the objective lens, causing, in turn, a continuous change in the focus of the image. Since the image is periodic, additional variation of focal length will provide a wide range of values, facilitating the detection of the best focus image. In the present case, 24 photomicrographs were taken to cover a range from -20 nm (overfocus) to $+300$ nm (underfocus) in which the Scherzer focus position is situated at a defocus of about 45 nm.

Although it has been stated that the present specimen is very radiation resistant, the molecules still cannot stand the total electron dose necessary for so many exposures for throughfocus imaging. The radiation damage on a crystalline specimen causes the diffraction spots to disappear gradually from the periphery towards the centre of the pattern. Harada *et al.*[16] have pointed out that the end point must be defined by the moment of disappearance of the reflections which correspond to the expected critical distance to be resolved in the final images. For the present specimen, this critical dose was measured to be about $2{\cdot}2 \times 10^6$ electrons nm^{-2} at the specimen plane. When this critical number of illuminating electrons was equally delivered to all throughfocus series, only a few seconds were available for a single exposure at a magnification of 200 000, giving the final optical density of 0·5 for the processed films. This situation resulted in considerable noise in each photomicrograph enhanced by the quantum fluctuation due to the deficiency in the number of recording electrons. In order to increase the signal-to-noise ratio, the final images were translationally averaged over the crystal periodicity along the direction of the *b*-axis of the image by applying a photographic multiple exposure technique.

Figure 7(a)–(d) gives some examples of these throughfocus images to show how drastically the actual images change their features with different focusing. In order to select the best focus image, a series of

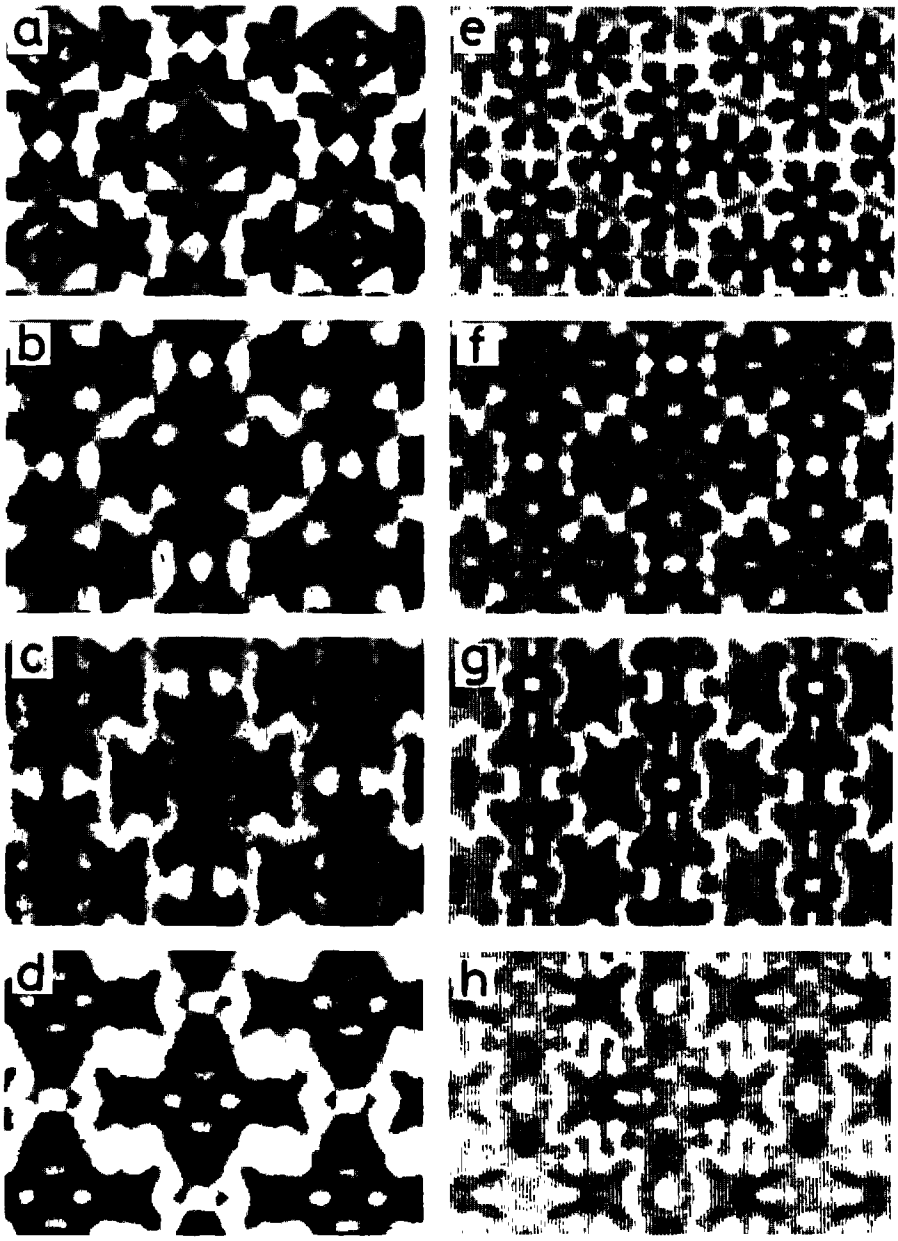

Fig. 7. Variation in image features by defocusing. (a–d) Real electron images and (e–h) theoretical images constructed by computer simulation. Defocus values: (a, e) 35nm; (b, f) 55 nm; (c, g) 100 nm; (d, h) 160 nm.

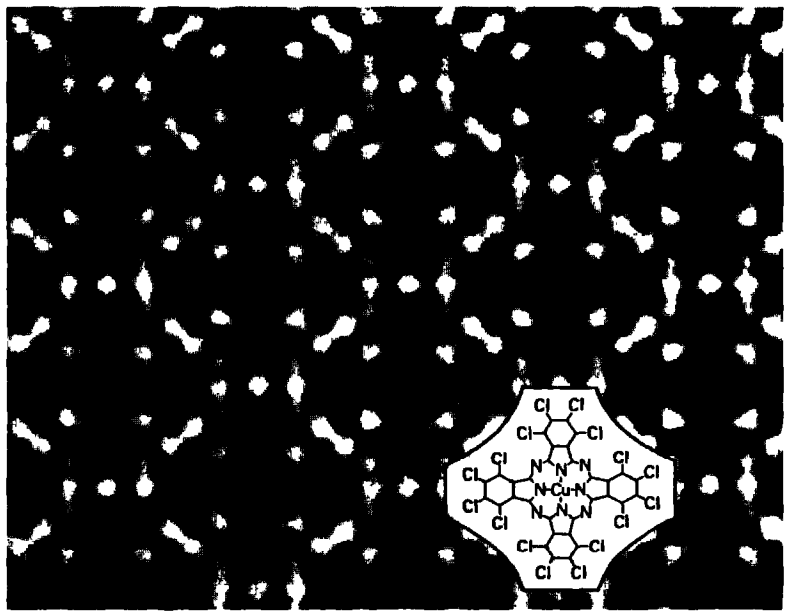

Fig. 8. High resolution molecular images of Cyanine Green taken with a 500 kV electron microscope at Kyoto University. Images due to Cu and Cl atoms are observable in addition to structural details such as benzene and azaporphyrin rings.

theoretical throughfocus images were constructed by computer simulation on the basis of the atomic parameters in the crystal as found by electron diffraction analysis and the characteristics of the objective lens; some of these images are collected in Fig. 7(e)–(h) to accord with the corresponding real images. By the comparison of both series, it was confirmed that the most reliable image is that which appears at the defocus position of 45 nm as predicted. Figure 8 is an enlargement of the image to show the details more clearly. The rhombic flower-like figures arranged in the face-centred rectangular array are the molecular images. When compared with the inset structure diagram, it is clearly recognized that the dark dots, one at the centre and the other 16 around each molecule, correspond to copper and chlorine atoms, respectively. It is often said that the full chlorination of Cu-phthalocyanine is rather difficult, although no chemical analysis was performed with the present specimen. As to the interpretation of the appearance of 16 chlorine atoms in each molecule, it must be taken into account that the images are given as the averaged structures due to the projection of molecular columns as well as due to the photographic signal enhancement processing.

The 16-membered azaporphyrin ring appears as a dark ellipse around the central copper atom supporting it with four links. Although not so clear, it is interesting to note that small rings surrounded by four chlorine atoms are also observed in some of the molecular images. Apparently, these rings reflect the structure of benzene rings within each set of four chlorine atoms. In the present case, the carbon and nitrogen atoms are not discriminated as clearly as the medium heavy atoms. This fact is also indicated theoretically by the computer simulation and is interpreted in terms of the low contrast of these light atoms.

5. THE RESOLUTION LIMIT AND RADIATION DAMAGE

It may be worthwhile to consider the applicability of high resolution imaging to ordinary organic materials which are more radiation sensitive than Phthalocyanine Green. The ultimate resolution attainable for a certain substance is closely dependent on its radiation resistance, which is usually defined in terms of the critical dose Q_c for high resolution. When the image is recorded on a photoplate with a sensitivity η to produce images of optical density γ after processing, the image resolution δ is given by

$$\delta = \left(\frac{\sigma^2}{\eta} \cdot \frac{\gamma}{pfQ_c}\right)^{1/2} \tag{6}$$

where σ is the diameter of silver grains, p is a constant and f is the ratio of electrons participating in image formation to those incident on the specimen. It is apparent from the equation that the resolution limit is inversely proportional to the square root of the critical dose, seemingly making it difficult to observe most organic compounds with atomic level resolution. Critical doses measured by various investigators are shown in Table 1. Since the measurements have been made under a variety of experimental conditions, including the instrument used, the specimen thickness, the incident beam current, the definition of the endpoint of damage, etc., the results may not be interpreted in any systematic sense. However, the listed data indicate a general tendency for the aliphatic hydrocarbons to be one order of magnitude less radiation resistant than the aromatic compounds and also that greater polycyclic condensation and full halogenation enhance the resistance. The ultimate resolution expected for each compound is also listed in the third column as a result of rough estimates based on empirical data. As to the aliphatic compounds,

TABLE 1
Critical Electron Dose for Various Organic Compounds and Expected Limits of Image Resolution

Substances	$Q_c(n_c\ nm^{-2})$	$\delta\ (nm)^a$	*Ref.*
Stearic acid	140	5·3	19
Paraffin	380	3·2	18
Polyethylene	470	2·9	18
Indigo	8 100	0·7	18
Tetracene	10 000	0·63	18
Bromanil	12 500	0·56	20
Coronene	15 000	0·51	18
Ag · TCNQ	18 800	0·46	17
Cyanine Blue	62 500	0·25	18
Hexabromobenzene	$1{\cdot}6 \times 10^5$	0·16	20
Cyanine Green	$2{\cdot}2 \times 10^6$	0·043	16

[a] Re-estimated by the present author.

even the molecular shape may not be recognized since the possible resolution is larger than the chain width. With aromatic compounds, however, it is expected that some skeletal groups such as benzene rings may be recognized as a whole, while full halogenation will make the molecule strong enough to reach atomic resolution. It is interesting to note that Phthalocyanine Green will give much finer structural detail only if the instrument acquires the capability to resolve it. The result of the present consideration, however, does not mean that finer resolutions than those predicted above are completely impossible, as the value of Q_c is defined in a statistical sense. If a great many photomicrographs are recorded, images with much finer resolution may be found to show the structural details.

Recently, the adoption of higher accelerating voltage is becoming a current trend in electron microscopy for the attainment of high resolution, so that the 200 kV instruments are manufactured as standard conventional products, possessing resolving power of nearly 0·2 nm or better. In order to reach the resolution estimated for each compound, the electrons of a critical dose must all be used for the image recording. Practically, however, additional electron irradiation is given to the specimen for other procedures such as the image field selection and focusing. Then, it is advisable to use a device which restricts the electron dosage only to the moment of image recording. The automated minimum

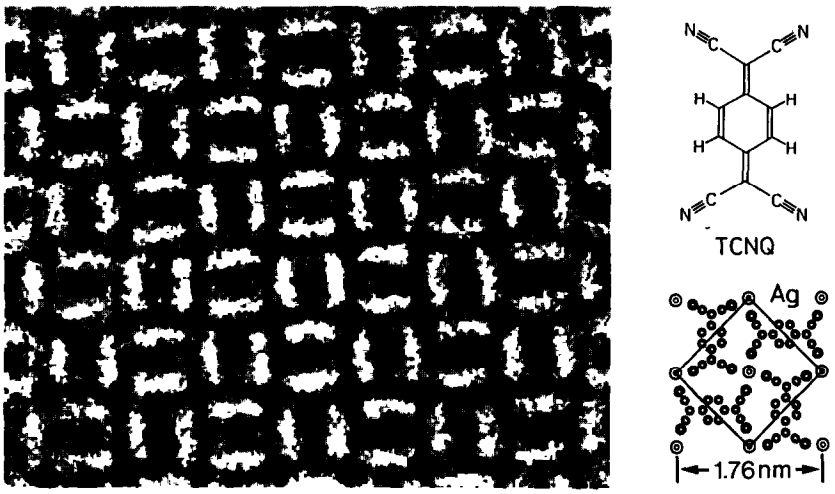

Fig. 9. High resolution molecular images of a charge-transfer complex of Ag · TCNQ taken with a conventional 200 kV electron microscope. Images due to Ag ion columns are observed at the knots of the net due to TCNQ molecules.

dose system (MDS) reported by Fujiyoshi *et al.*[21] is an example of a device of this kind. Generally, the focusing is performed on a small area near the target image field which is subsequently exposed to the total illumination for the photo recording. The size and the position of the illuminated area as well as the direction and divergence of the beam can be varied by the combined control of beam deflectors and condenser system. Since the whole procedure is rather complicated, the system is designed so as to be operated with the aid of a computerized circuit including the setting of the exposure time, the illuminating beam current, and so on. In this case, the focusing is subjected to visual trial and the selection of target area should be done under extremely low illumination.

As an example of performance with a conventional 200 kV instrument,[17] the high resolution electron photomicrograph of an Ag · TCNQ crystal is reproduced in Fig. 9 to show the arrangement of projected Ag ion columns and TCNQ molecules. As is apparent from comparison with the inserted structure diagram, it is clear that the N≡C—C—C≡N chains form a square zig-zag net and Ag ion columns are located at the knots of the net. The benzene rings appear as slightly oblong figures alternatively oriented in the net pointing to two different directions normal to each other. The present result fairly well reflects the estimation of resolution listed in Table 1.

If the critical dose Q_c is increased by an order of magnitude, the resolution may be improved by nearly threefold—so as to match the limit of the conventional instrument. At present, however, the only possible way is considered to be to cool the specimen down to 4·2K by the use of a liquid helium cryostage, since the radiation damage is caused by two major processes, the ejection of orbital electrons by the excitation and the breaking of C—H bonds by collision of electrons. In any case, the reaction rate of molecular decomposition may be exponentially reduced at very low temperature. On the basis of this principle, the development of a cryomicroscope is under progress with a view to further improvement of resolution for organic materials including biological macromolecules.

6. CONCLUSION

It is apparent from the above observations that the images of atoms have been recorded without ambiguity. The results are considered to render a new human experience to confirm the presence of atoms by visual inspection. However, it is important to identify the status of these images in relation to the actual reality of the object material. The electron waves which convey the information about atoms are scattered by the electrostatic potential in each atom. Hence, the image which is supposed to be the atom simply reflects the distribution of atomic potential and not the solid entity of the atom. In this sense, the situation is similar to the X-ray diffraction case, where the final 'image' is given as the electron density map of each atom. Since there is at present no way directly to form images other than by electron waves, these images so far observed cannot but be accepted as reflecting the reality as far as the capability of electron microscopy is concerned in general. Whatever the physical meaning might be, high resolution imaging at atomic level is currently adopted as the direct approach to investigate not only regular structures but the commonly irregular configurations in every field of natural science.

ACKNOWLEDGEMENT

The author wishes to thank Professor I. D. Rattee of the University of Leeds, England, and Dr H. M. Smith of Sun Chemical Corporation, USA, for their special interests in the present work.

REFERENCES

1. J. M. Robertson, *Organic Crystals and Molecules*, Ithaca, New York, Cornell University Press (1953).
2. J. W. Menter, *Proc. Roy. Soc. London*, **A236**, 119 (1956).
3. N. Uyeda, T. Kobayashi, E. Suito, M. Watanabe and Y. Harada, in: *Proc. 7th Int. Congr. Electron Microsc.*, Vol. 1, ed. P. Favard, Paris, Societé Français de Microscopie Electronique, 1970, p. 23.
4. O. Scherzer, *J. Appl. Phys.*, **20**, 20 (1949).
5. T. Kobayashi, E. Suito, N. Uyeda, M. Watanabe, M. Yanaka, T. Etoh, H. Watanabe and M. Moriguchi, in: *Proc. 8th Int. Congr. Electron Microscopy*, Vol. 1, eds J. V. Sanders and D. J. Goodchild, Canberra, Australian Academy of Science, 1974, p. 30.
6. N. Uyeda, M. Ashida and E. Suito, *J. Appl. Phys.*, **36**, 1453 (1965).
7. M. Ashida, N. Uyeda and E. Suito, *Bull. Chem. Soc. Japan*, **39**, 2632 (1966).
8. N. Uyeda, Y. Murata, T. Kobayashi and E. Suito, *J. Cryst. Growth*, **26**, 267 (1974).
9. N. Uyeda and Y. Murata, *J. Cryst. Growth*, **57**, 551 (1982).
10. T. Kobayashi and N. Uyeda, in: *Proc. 9th Int. Congr. Electron Microsc.*, Vol. 1, ed. J. Sturgess, Toronto, Microscopical Society of Canada, 1978, p. 300.
11. H. Saijo, N. Uyeda and E. Suito, *J. Chem. Soc., Farad. Trans. II*, **73**, 740 (1977).
12. J. M. Cowley and A. F. Moodie, *Acta Crystallogr.*, **10**, 609 (1957).
13. K. Ishizuka and N. Uyeda, *Acta Crystallogr.*, **A33**, 740 (1977).
14. N. Uyeda, T. Kobayashi, E. Suito, M. Watanabe and Y. Harada, *J. Appl. Phys.*, **43**, 5181 (1972).
15. N. Uyeda, T. Kobayashi, K. Ishizuka and Y. Fujiyoshi, *Chemica Scripta*, **14**, 47 (1978/79).
16. Y. Harada, T. Taoka, M. Watanabe, M. Ohara, T. Kobayashi and N. Uyeda, in: *Proc. 30th Ann. Meeting EMSA*, ed. C. J. Arceneaux, Baton Rouge, LA, Claitor's Publish. Div., 1972, p. 686.
17. N. Uyeda, T. Kobayashi, K. Ishizuka and Y. Fujiyoshi, *Nature*, **287**, 755 (1980).
18. M. S. Isaacson, in: *Principle and Technique of Electron Microscopy*, Vol. 7, ed. M. A. Hayat, New York, Van Nostrand Reinhold Co., 1976, p. 1.
19. J. Dubochet and E. Knapek, *Chemica Scripta*, **14**, 267 (1978/79).
20. T. Kobayashi and L. Reimer, *Bull. Inst. Chem. Res. Kyoto Univ.*, **53**, 105 (1975).
21. Y. Fujiyoshi, T. Kobayashi, K. Ishizuka, N. Uyeda, Y. Ishida and Y. Harada, *Ultramicrosc.*, **5**, 459 (1980).